NATIONAL INSTITUTE FOR FUSION SCIENCE

Internal Transport Barrier Simulation in LHD

J. García, K. Yamazaki, J. Dies, J. Izquierdo

RESEARCH REPORT
NIFS Series

TOKI, JAPAN

Internal Transport Barrier Simulation in LHD

J. García [1], K.Yamazaki [2], J. Dies [1], J.Izquierdo [1]

1. *Fusion Energy Engineering Laboratory (FEEL),Departament de Física i Enginyeria Nuclear, ETSEIB, Universitat Politècnica de Catalunya (UPC), Barcelona (Spain).*
2. National Institute for Fusion Science, Toki, Gifu, 509-5292, Japan.
(Present Address: Nagoya University, Chikusa-ku, Nagoya 464-8603 Japan)

In order to study the electron heat transport channel and to clarify the electron thermal diffusivity dependence with some plasma parameters in LHD shots with internal transport barrier (ITB), some transport models have been added to TOTAL code. These models can be divided into two categories: Bohm and GyroBohm-like models and drift wave models. A sketch of mixed short and long wavelength models has been derived for this study as a good candidate for the ITB explaining.

The effect of anomalous transport reduction by the electric field shear has been introduced by means of the factor $\left(1+(\tau\omega_{ExB})^{\gamma}\right)^{-1}$. This factor has been previously checked as a good candidate to drive anomalous transport in tokamak plasmas.

Results show that a combination of short wavelength and long wavelength together with the electric field shear can explain the transition between non-ITB and ITB shots. The central temperature dependence with density is also well simulated. In the case of GyroBohm models, they fit also temperature profiles, although central temperature dependence with density is higher.

---

1. Introduction

Low temperatures and low confinement is usually achieved in confined plasmas due to the high heat transport caused by turbulence. However, high electron temperature plasmas with peaked profiles have been obtained in the Large Helical Device (LHD) [1] as well as in others stellarator devices, as the Compact Helical System (CHS) [2] and the TJ-II [3]. Theses scenarios have been named Internal Transport Barrier (ITB) scenarios. These shots share the common characteristic of having a high positive electric field in the plasma core with a large shear. Both, electric field and its shear are supposed to suppress neoclassical transport and anomalous one, respectively.

Different from tokamaks electron transport barrier scenarios (where magnetic field shear seems to play a significant role), transition between ion root (large neoclassical flux with small electric field (E_r)) to electron root (small neoclassical flux with a large positive E_r) in the plasma core seems to drive the transport barrier in stellarators [4] when collisionality is low enough [5]. These facts are related strongly to the appearance of a density limit, below which, ITB is formed. Besides, the power deposition profile, as well as, ion temperature profile, seems to be important for the ITB formation.

In order to study the electron heat transport channel and to clarify the electron thermal diffusivity dependence on some plasma parameters in LHD shots with internal transport barrier (ITB), some transport models have been added to TOTAL [6] code. These models can be divided into two categories: Bohm and GyroBohm-like models and drift wave models. A sketch of mixed short and long wavelength models has been derived for this study as a good candidate for explaining the ITB. The effect of anomalous transport reduction by the electric field shear will be analyzed too.

The Bohm and GyroBohm-like models used in this paper are inspired from the Joint European Torus (JET), mixed-model [7], shown later as Eq. 3 in Chapter 4. Generally speaking, the Bohm models establish that the electron heat diffusivity has the form $\chi_e \propto T_e$,

and the GyroBohm $\chi_e \propto T_e^{3/2}/L$ where T_e is the electron temperature and L is the characteristic length of the reactor device. Physically speaking, the two models clearly distinguish the size of the convective cells formed by turbulence. The Bohm scaling arises from the mesoscale with characteristic length $\Delta x = (\rho_s L_T)^{1/2}$ where $\rho_s = (m_i T_e)^{1/2}/eB$ and $L_T^{-1} = |\nabla(ln T_e)|$. When the convective cell size reduces to scale as $\Delta x = \rho_s$ the GyroBohm scaling is applied.

These models have been empirically deduced to explain the electron temperature of tokamak plasmas in the turbulent mode, and have been broadly checked in the JET. Later, some improvements (as electron temperature gradient dependence) have been added in order to explain the enhanced confinement scenarios.

On the other hand, drift wave model can be divided into short (called electromagnetic drift waves) and long wavelength (called electrostatic drift waves) models Eq.4, 5, 6. The long wavelength drift wave models arise from the fluctuations of the electric field of the plasma and the short ones arise from the fluctuations of the magnetic field. The characteristic length of the electrostatic waves, $\Delta x_{es} = q\rho_s \dfrac{R}{L_T}$, is similar to the size of the convective cells of the GyroBohm scaling, and actually, both models are closely related leading to similar predictive results. Contrary to the long pattern of the electrostatic drift waves, the short wavelength have lead to coherent structures of the collisionless skin depth $\Delta x_{em} = c/\omega_{pe}$, where c is the light speed and $\omega_{pe} = \sqrt{n_e e^2/\varepsilon_0 m_e}$ is the plasma frequency. In a typical tokamak, this length is of order of a few millimeters and is much smaller than long wave that is on the scale of several centimeters [8]. Studies of electron transport in the spectrum range of the electromagnetic waves show the stochastization of the guiding center orbits and the fast propagation of the electron heat flux with small correlation time [9].

Analyzing the mixing lengths Δx_{es} and Δx_{em} one can find that both type of transport can exits in the plasma. The condition $\Delta x_{es} = \Delta x_{em}$ leads to the expression for the plasma beta $\beta_{crit} = L_T^2/q^2 R^2$ at the transition between the two regimes. Therefore, in a plasma with ITB, where the electron temperature is very high in the plasma core and the electron

3

density profile is almost flat, the β_{pe} may be higher than β_{crit} at the plasma core and lower outside that region. In order to study whether these tokamak ideas may be applied to stellarators a sketch of mixed short and long wavelength models has been derived for this study (Eq.7) as a good candidate for the reduction of the turbulence to the ITB levels.

The effect of anomalous transport reduction by the electric field shear has been introduced by means of the factor $1 / \left(1 + (\tau \omega_{ExB})^{\gamma}\right)$ as described in Eq.8. This factor has been previously checked as a good candidate to drive anomalous transport in tokamak plasmas [10], as well as, also derived from theoretical models [11,12].

In addition to this, a non-local transport model, Eq. 10, has been used to study how a model of this kind can reproduce steady-state shots with and without ITB.

The aim of this study is, to search for best models that reproduce a LHD ITB shot, and show their dependence with electron density, in order to obtain the critical behavior previously described. By using these best fitted transport models, we might easily extrapolate the present data to the future reactor plasmas design.

2.Experimental set-up

The shot analyzed (#26943) corresponds to the fifth campaign of the LHD experiment, the high peaked electron temperature profile has been obtained by using 1 MW of Electron Cyclotron Heating (ECH) heating power [13]. Figure 1 shows the electron temperature and density profile measured by 200-channel YAG Thomson scattering system [14] and 11-channel FIR interferometer [15]. The density profile was obtained by Abel inversion method with 3-dimensional self-consistent equilibrium calculated by using extended radial magnetic coordinates to treat with ergodic regions in the PRE-TOTAL code.
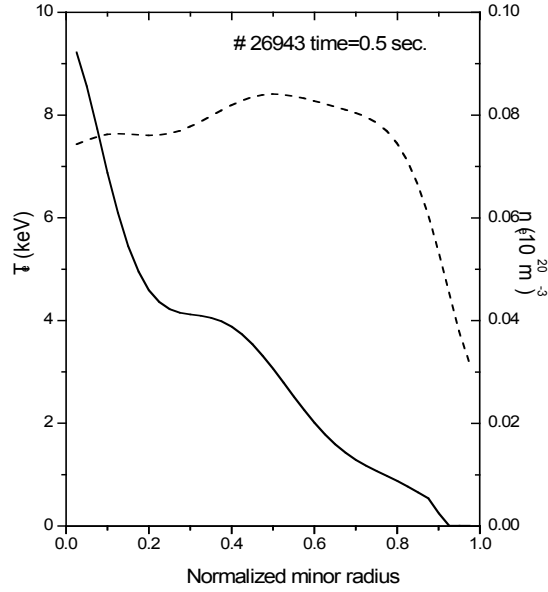
Figure 1 Experimental profiles of electron temperature and density obtained in LHD

The central ion temperature is measured by the crystal spectrometer measurement, and the plasma equilibrium is calculated by assuming ion temperature profile.

Related to the power deposition profile, it is modelled by the following power localization to the central region with the width of $\rho_{wid} = 0.1$:

$$P_{ECH} \propto \frac{1}{\exp\left[\left(\rho/\rho_{wid}\right)^4\right]},$$

which roughly agrees with the results of the ray-tracing analysis.

3. Model equations for neoclassical transport

Neoclassical transport in helical systems is divided into an axisymmetric tokamak-like part [16,17] and an asymmetric helical part [18,19]. The radial flux coordinate is defined as $r = \left(\phi/\phi_0\right)^{1/2}$, where ϕ is the toroidal magnetic flux. The expression for the radial

5

asymmetric neoclassical flux associated with helical-ripple trapped particles Γ_j^{na} and heat flux Q_j^{na} of electrons (j=e) and ions (j=i) is given as:

$$\Gamma_j^{na} = -\varepsilon_t^2 \varepsilon_h^{1/2} v_{dj}^2 n_j \int_0^\infty x^{5/2} e^{-x} \tilde{v}_j \frac{A_j(x, E_r)}{\omega_j^2(x, E_r)} dx$$

$$Q_j^{na} + \frac{5}{2}\Gamma_j^{na} T_j = -\varepsilon_t^2 \varepsilon_h^{1/2} v_{dj}^2 n_j T_j^2 \int_0^\infty x^{7/2} e^{-x} \tilde{v}_j \frac{A_j(x, E_r)}{\omega_j^2(x, E_r)} dx$$

where

$$x = m_j v^2 / 2T_j$$

$$A_j(x, E_r) = n_j' / n_j - Z_j e E_r / T_j + (x - 3/2) T_j' / T_j$$

$$\tilde{v}_j(x) = v_j^0 x^{-1.5} \varepsilon_h^{-1} \left\{ \left[(1 - 1/2x) erf(x^{1/2}) + \frac{e^{-x}}{(\pi x)^{1/2}} \right] + \bar{Z}_j \right\}$$

$$\omega_j^2(x, E_r) = 4.21\tilde{v}_j^2 + 1.5(\varepsilon_t/\varepsilon_h)^{1/2}(\omega_E + \omega_{Bj})^2 + (\varepsilon_t/\varepsilon_h)^{3/2}\left[\frac{\omega_{Bj}}{4} + 0.6|\omega_{Bj}|\tilde{v}_j(\varepsilon_t/\varepsilon_h)^{3/2} \right]$$

Here ε_t is the toroidal inverse aspect ratio, ε_h is the helical ripple modulation, n_j is the plasma density, T_j is the plasma temperature, v_{dj} is the thermal velocity, ω_E is the *ExB* drift, ω_B is the ∇B drift frequency. The prime denotes the derivative with respect the radial coordinate.

The total particle flux is

$$\Gamma_j^t = \Gamma_j^{sym} + \Gamma_j^{na} - D_a \left\langle |\nabla r|^2 \right\rangle \frac{\partial n_j}{\partial r}$$

where D_a is the anomalous particle diffusivity and Γ_j^{sym} is the symmetric neoclassical particle flux . The total heat flux is defined as

$$Q_j^t = Q_j^{sym} + Q_j^{na} - n_j \chi_a \left\langle |\nabla r|^2 \right\rangle \frac{\partial T_j}{\partial r}$$

6

where χ_a is the anomalous heat diffusivity and Q_j^{sym} is the symmetric neoclassical heat flux.

With the aim of studying the evolution of electron and ion temperatures by keeping clear the role played by density, this late parameter has been kept fixed, therefore the equations solved in this paper are:

$$\frac{\partial(n_e T_e)}{\partial t} = -\frac{1}{V'}\frac{\partial}{\partial r}\left(V'Q^t\right) - \frac{m_e}{m_i}\frac{n_e}{\tau_e}(T_e - T_i) - P_{rad} + P_{add}$$

where τ_e is the electron collision time. The second term of the right hand side is the heat exchange between ions and electrons, the third one represents radiation losses, mainly bremmstrahlung radiation, and the last one is ECRH heating.

A similar equation is solved for ions:

$$\frac{\partial(n_i T_i)}{\partial t} = -\frac{1}{V'}\frac{\partial}{\partial r}\left(V'Q^t\right) + \frac{m_e}{m_i}\frac{n_e}{\tau_e}(T_e - T_i)$$

In this case no heating deposition is considered for ions, according to experimental set up.

4. Anomalous transport models

The following list contains the models used along this study:

1. GyroBohm-like model: $\chi_e = \alpha_e^{gB}\chi_{gB}$, $\chi_{gB} = (cT_e/eB)(\rho_i/L_{Te})$, $L_{Te} = \left|\frac{\nabla T_e}{T_e}\right|^{-1}$

2. Bohm-like model $\chi_e = \alpha_e^{B}\chi_B$, , $\chi_B = (cT_e/eB)(q^2 a/L_{Pe})\langle L_{Te}\rangle^{-1}$, $L_{Pe} = \left|\frac{\nabla P_e}{P_e}\right|^{-1}$,

$$\langle L_{Te}\rangle^{-1} = \left|(T_e(\rho = 0.8) - T_e(\rho = 1))/T_e(\rho = 1)\right|$$

3. Mixed Bohm-GyroBohm $\chi_e = \alpha_e^{gB}\chi_{gB} + \alpha_e^{B}\chi_B$, $\chi_{gB} = (cT_e/eB)(\rho_i/L_{Te})$,

$$\chi_B = (cT_e/eB)(q^2 a/L_{Pe})\langle L_{Te}\rangle^{-1}, L_{Pe} = \left|\frac{\nabla P_e}{P_e}\right|^{-1}, L_{Te} = \left|\frac{\nabla T_e}{T_e}\right|^{-1},$$

$$\langle L_{Te}\rangle^{-1} = \left|(T_e(\rho = 0.8) - T_e(\rho = 1))/T_e(\rho = 1)\right|$$

4. Short wavelength (Sw1) $\chi_e = C_1(r/R)^{1/2}\dfrac{v_{the}}{R}\dfrac{c^2}{\omega_{pe}^2}$

5. Short wavelength (Sw2) $\chi_e = C_1\dfrac{v_{the}}{(L_{Te}R)^{1/2}}\dfrac{c^2}{\omega_{pe}^2}$

6. 6-Regimes drift wave

7. Mixed short wavelength long wavelength model

$$\chi_e = C_1(r/R)^{1/2}\frac{v_{the}}{R}\frac{c^2}{\omega_{pe}^2}\theta(\beta_{crict}) + (1-\theta(\beta_{crict}))C_2(cT_e/eB)(\rho_i/L_{Te})$$

8. Internal transport barrier model $\chi_{e,shear} = \dfrac{\chi_e}{1+(\tau\omega_{ExB})^\gamma}$, where $\omega_{ExB} = \partial_r(E_r/B_\theta)$

   with E_r the plasma radial electric field and B_θ the poloidal magnetic field. The following values τ =5.5 s, γ =1.5 have been used throughout this study. The constant τ can be seen regarded as the correlation time for the fluctuations without ExB flow.

9. OHE model (long wavelength-like, GyroBohm)

$$\chi_i = C(cT_e/eB)q^2(\rho_i/L_T)(R/L_T)^{3/2}$$
$$\chi_e = \chi_i\varepsilon^{1/2}$$

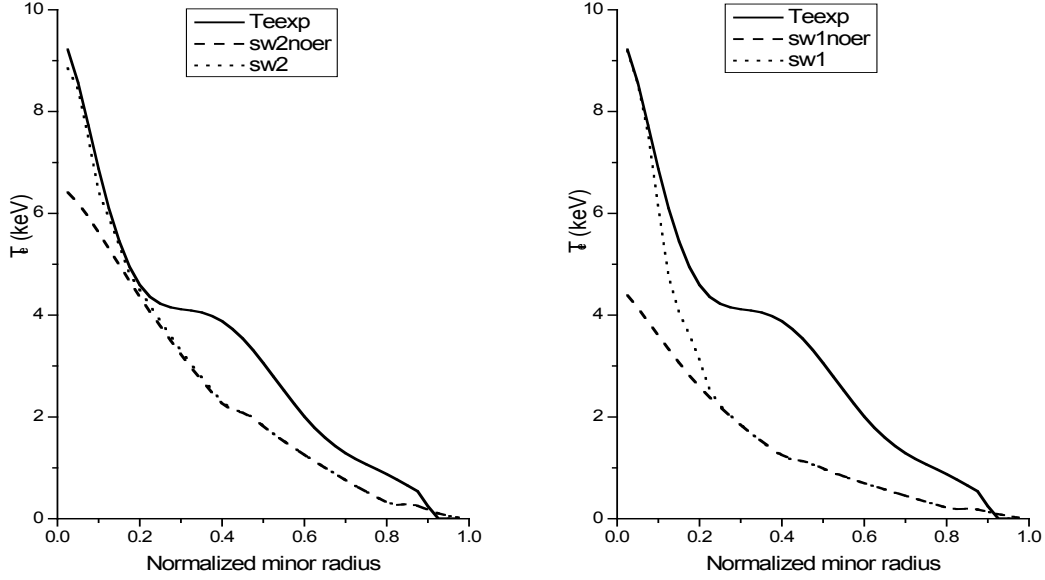## 5. Simulation results

5.1 Drift wave models

Figure 2 Comparison between short wavelength sw2 (left, eq. 5), short wavelength sw1 (right, eq.4) and experimental electron temperature profile, with and without electric field shear effect.

In figure 2 and figure 3 the electron temperature profiles for the models Sw1, Sw2 and 6-regime drift wave with and without electric field shear effect are compared with the experimental electron temperature. From the figures, one can see that short wavelength models (in particular sw2) can reproduce the temperature profile in the plasma core in the range $0 \leq \rho < 0.2$. However, outside this range, the plasma profiles are completely wrong, with temperatures quite different from the experimental ones. In this situation, one can think about the existence of a transition between one kind of transport in the plasma core and another type outside this zone. This point will be clarified along this study.

Related to the electric field shear effect, the electron temperature profiles become peaked (a high electron temperature gradient appears at the plasma core) and higher central electron temperature are obtained by means of the introduction of this effect in the calculation, whereas the rest of the plasma profile is very similar in both situations.
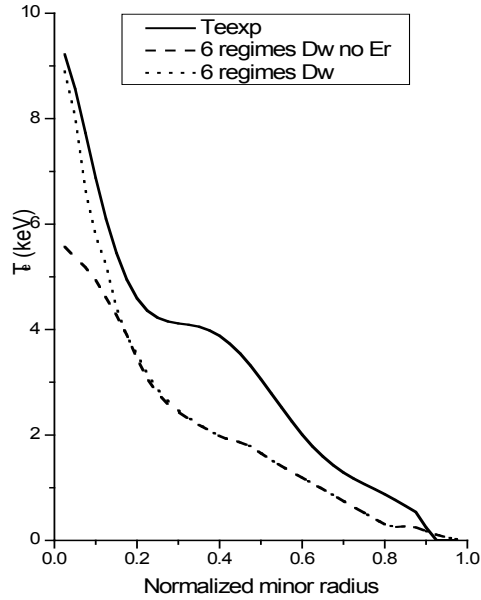
9

Figure 3 Comparison between 6-regimes drift wave and experimental electron temperature profile, with and without electric field shear effect

5.2 Bohm and Gyro-Bohm like models

In figure 4 and figure 5 the electron temperature profiles for three models, Bohm, GyroBohm and mixed model with and without electric field shear effect, are compared with the experimental electron temperature. First of all, one can see from the figures that all the three models lead to similar results. This is due mainly to the fact that in this scenario (with almost flat density profile) the values of the factors L_{T_e} (from the GyroBohm model) and L_{P_e} (from the Bohm model) are very similar, however GyroBohm model tends to give a flater profile outside the core plasma.
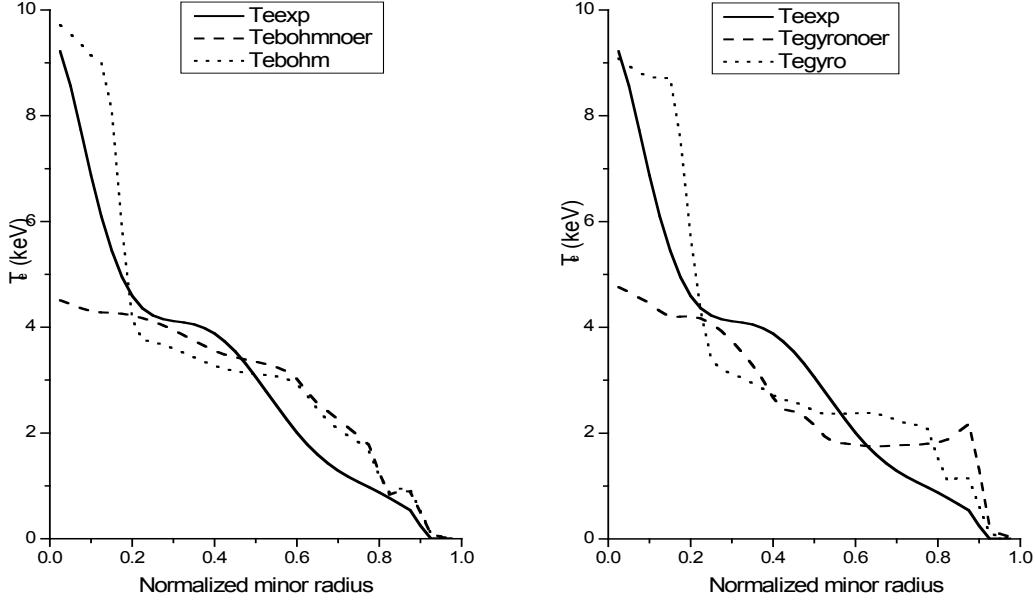
Figure 4 Comparison between Bohm-like (left, eq. 2), GyroBohm-like (right, eq.1) and experimental electron temperature profile, with and without electric field shear effect

The central temperature profile obtained with these models has a more parabolic shape compared to the drift wave models and the temperature gradient in the region $0 \leq \rho < 0.1$ is much smaller. However a high gradient (comparable to the ones obtained in the drift wave profiles) is obtained in the region $0.1 \leq \rho < 0.2$. These values of the temperature are compatible with the experimental values and always fit within the error bars.

The main difference between these models and the ones studied in the previous section is that outside the plasma core (where the influence of the electric field shear is negligible) these models reproduce the experimental profiles with reasonable accuracy. Moreover, the transition point (between a region with high temperature gradient and a small one) observed in the experimental profile at $\rho \approx 0.2$ is well simulated.

Clearly, one can see that the influence of the electric field shear on the profiles is stronger in this case than in the drift wave scenarios. This is due to the fact that the electric field obtained has a higher shear in this case and its effect over a quite flat temperature profile is stronger than in the case of drift wave, where the electron temperature gradient is always high at the plasma core even without electric field shear.
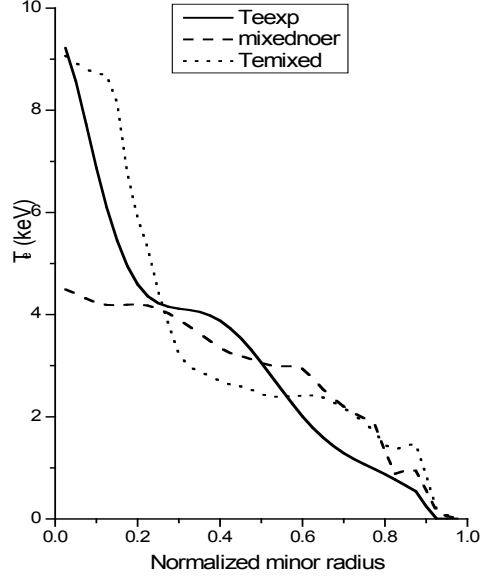
Figure 5 Comparison between Mixed Bohm-GyroBohm (eq. 3), and experimental electron temperature profile, with and without electric field shear effect.

5.3 Mixed drift wave models

In section 5.1 it has been shown that a model based in short wave length can simulate the ITB LHD shot #26943 in the region $0 \leq \rho < 0.2$, however it seems more adequate a long wavelength based model to simulate the plasma electron temperature outside this region. With the aim of having a global transport model, a combination of short wavelength a long wavelength drift model has been derived in this study (Eq.7). The transition between both regimes depends of the parameter $\beta_{crict}(\rho)$. As a first step using this model, this value has been imposed to get the transition point at $\rho = 0.2$. In next sections, it will be calculated using the condition that the characteristic length of both models is same.

From figure 6, one can see that the simulated profile has a steep gradient in the plasma core and a more flat shape at the edge. The high peaked gradient is due to two effects coupled: first, that the high sheared electric field obtained using this model reduces electron anomalous heat transport and the other that the short wavelength model is an Electron Tempearture Gradient (ETG) like model and this type of thermal flux enhances the appearance of high electron temperature gradients along the plasma due to the

12

existence of short coherent structures. However, in this case such high gradients are limited by the transport model because of their limitation to the range $0 \leq \rho < 0.2$. Outside this region, the gradients are softer, and as can be seen from figure 6, the simulated profile fits reasonably well the experimental one.
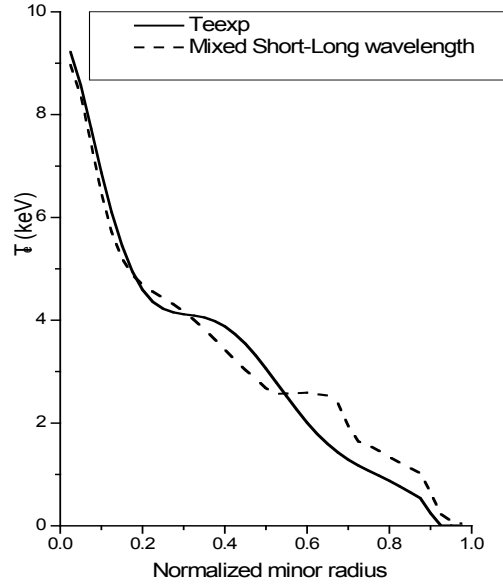

Figure 6 Comparison between mixed short wavelength long wavelength model (eq. 7), and experimental electron temperature profile.

6. Density study

The ITB formation in plasmas is strongly linked with the average density. In the LHD plasmas, it has been experimentally shown that exits a critical density below which (and if the power deposition centred enough) the ITB is formed. In order to study the validity of the previous transport models, not just for one shot with ITB, but for a wide range of plasma parameters, with the aim of reproducing the critical transition between a non-ITB scenario and an ITB one, some simulations have been carried out with the same electron density profile than in the previous section but with different average densities.

The electron density profiles are given in figure 7 (left) and the average density of each profile in table 1.

Density profile	Average density (x 10^{20} m^{-3})
1	0.07
2	0.09
3	0.11
4	0.22
5	0.32
6	0.52

Table 1 Average electron densities used in the density study.

The first model applied is the mixed short wavelength long wavelength model. As a first step and in order to see the importance of the factor β_{crict}, it has been kept fixed along the simulations, and its value is the same one as used for the ITB shot. This corresponds to the situation which has the transition point between the two regimes at $\rho = 0.2$. The results are given in figure 7 (right) and, as can be seen, although the ITB shot is well simulated, there is no clear transition between ITB and non-ITB scenarios because of the lack of a critical transition between high peaked temperature profiles with high electron temperature gradients and temperatures profiles with small gradients.

It is worth to point out that in the high densities scenarios, which have small negative electric field values at the plasma core (and consequently there is no clear anomalous transport suppression), high temperature gradients are obtained in the range $0 \leq \rho < 0.6$. This situation confirms the results about short wavelength model obtained in the previous section, which showed that this model tends to make the electron temperature profiles to have relatively high gradients even with no electric field shear suppression.
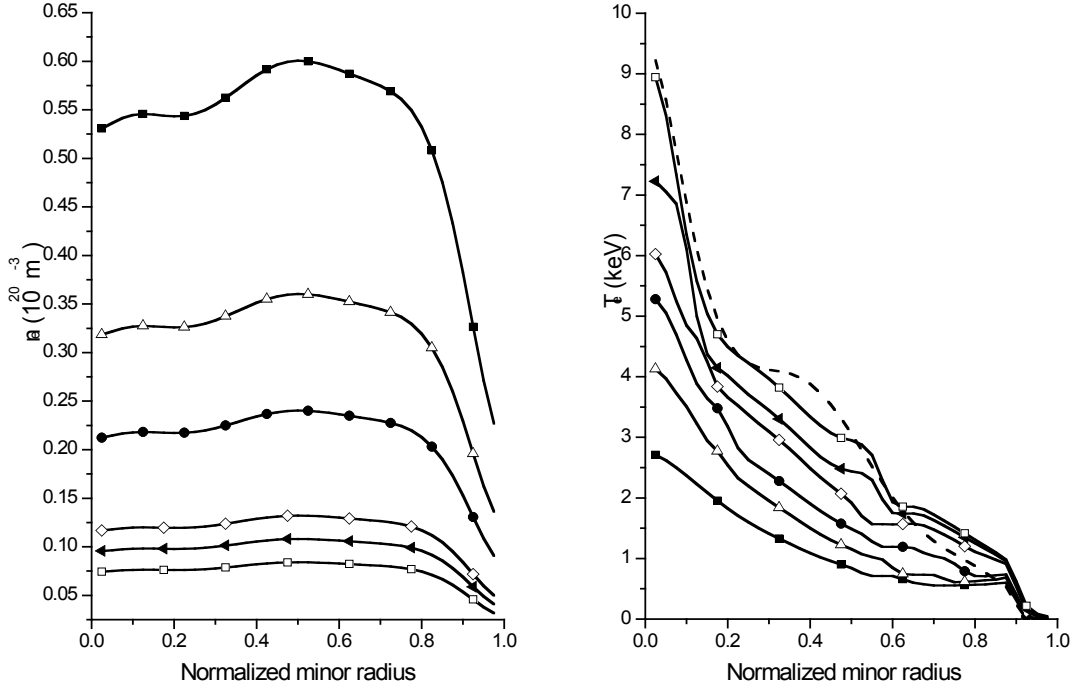
Figure 7 Density profiles used along the simulations (left). Electron temperature profiles (right) obtained with equation 7 and fixed β_{crict} (the same one than the original shot)

In order to avoid this behaviour, the transition point β_{crict} has been calculated imposing the condition that the characteristic lengths of both type of transport are similar. This condition leads to expression $\beta_{crit} = L_T^2/q^2 R^2$ for the critical beta. The electron temperature profiles obtained, using this value in equation 7, are shown in figure 8 (left).

In this case, a clear transition between some scenarios with ITB and some ones without ITB is obtained. The critical transition is obtained for an average density $<n_e> \approx 0.2x10^{20} m^{-3}$. In order to analyze the central electron temperature dependence on the average density, both variables have been plotted in figure 9 (left). There are two regimes quite different. The first one, corresponding to ITB scenarios, has temperature dependence $T_e(0) \propto <n_e>^{-0.57}$, whereas in non-ITB scenarios, this dependence is $T_e(0) \propto <n_e>^{-0.39}$. Clearly, the temperature dependence of density in ITB cases is stronger.
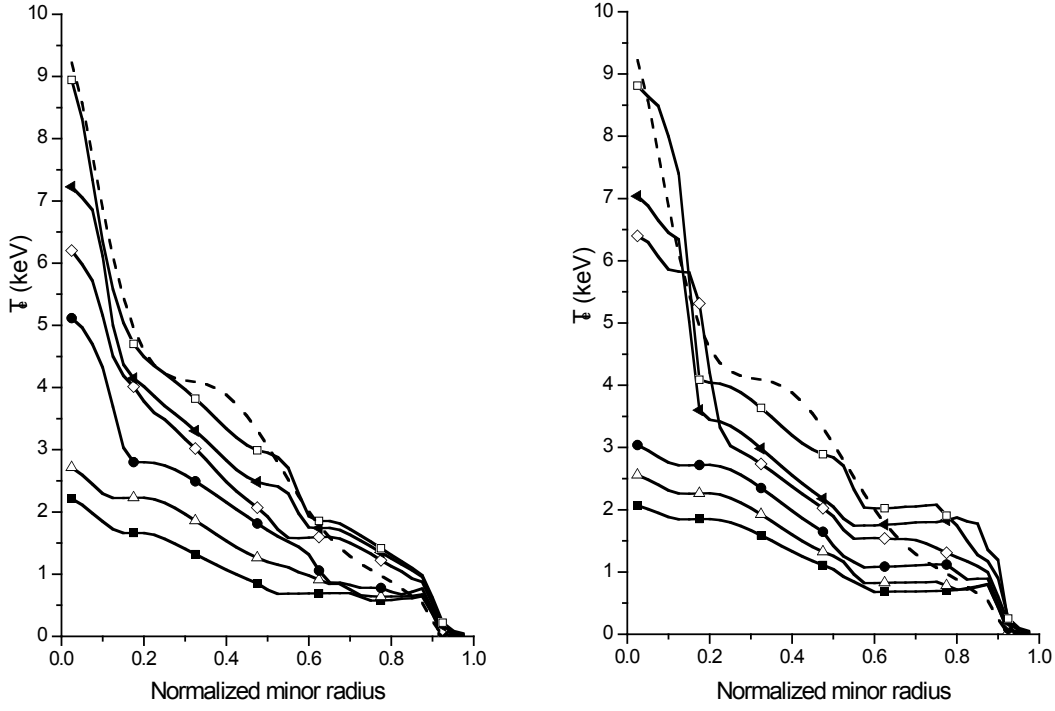
Figure 8 Electron temperature profiles obtained with equation 7 (left) and variable β_{crict}. Electron temperature profiles obtained with equation 1 (right)

Comparing these results with experimental data [1], one can conclude that this model, with this experimental set-up, can simulate the plasma behaviour with reasonable accuracy.

Finally, a complete GyroBohm-like scaling (Eq.1) has been applied to analyze its dependence with density. The profiles obtained as well as the central electron tempenrature dependence on the average density are shown in figure 8 (right) and 9 (right) respectively. In this case a similar behaviour is obtained, although the central temperature profiles seem to be more "parabolic". The critical density is now lower, $< n_e > \approx 0.1x10^{20}m^{-3}$, than the previously one obtained. The central temperature dependence on average density is $T_e(0) \propto < n_e >^{-0.72}$ in the ITB case and $T_e(0) \propto < n_e >^{-0.42}$ in the non-ITB one. Therefore, we can deduce that outside the core regions, both transport models lead to similar results, but in the plasma core the dependence of the GyroBohm-like model is much stronger. This fact makes the critical transition to be steeper and clearer but not similar to the experimental evidence. Anyway,

this dependence should be clarified with more experimental results to decide which type of transport is dominant at the plasma core in the case of ITB shots.
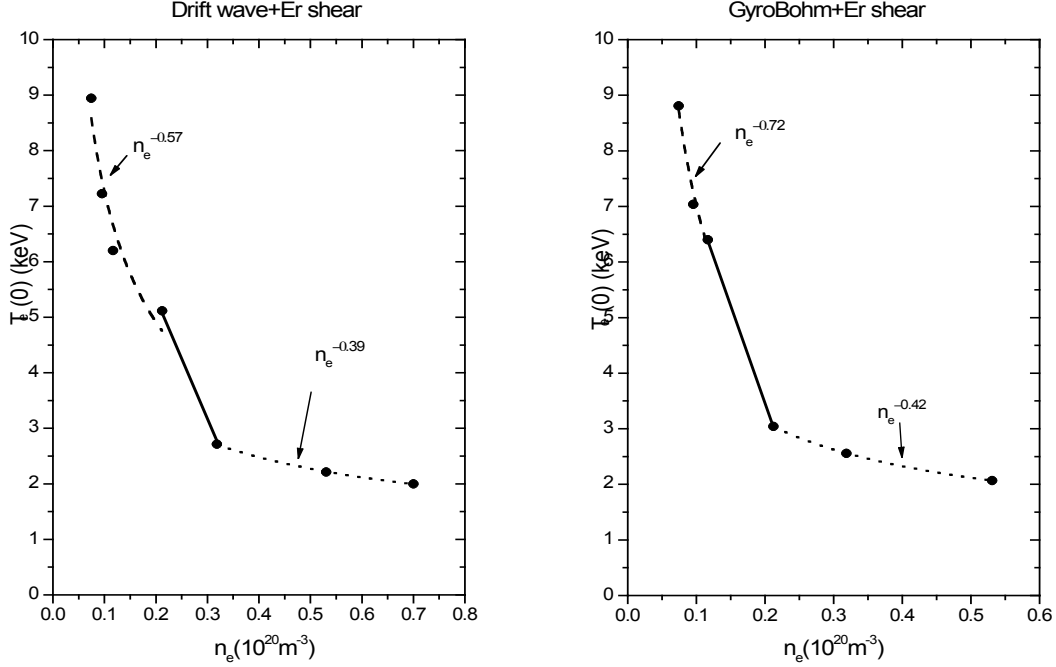

Figure 9 Central electron temperature dependence with density obtained for eq. 7 (left) and eq. 1 (right)

7. Analysis of the electric field and electron thermal diffusivity

In order to analyze the previous results, not just comparing the experimental temperature profile, but some more variables, a comparison of the electric field and the electron thermal diffusivity has been carrying out for the shot #26943 of the LHD. The electric field is calculated using the ambipolar condition, $\Gamma_e^{asym} = \sum_k Z_k \Gamma_k^{asym}$, where Γ_e^{asym} is the asymmetric part of the neoclassical electron flux, Γ_k^{asym} and Z_k are the asymmetric neoclassical ion flux and the ion charge for each species k respectively.

The electric field and thermal diffusivities profiles for the mixed drift wave case are given in figure 10, and for the GyroBohm-like model in figure 11. The electric field for both simulations is quite similar, with a high central value $E_r \approx 750$ V/cm and high electric

17

field shear $|dE_r/dr| \approx 125$ V/cm^2. In the outer part of the plasma, the electric field tends to be small with either positive or negative values and very small electric field shear.
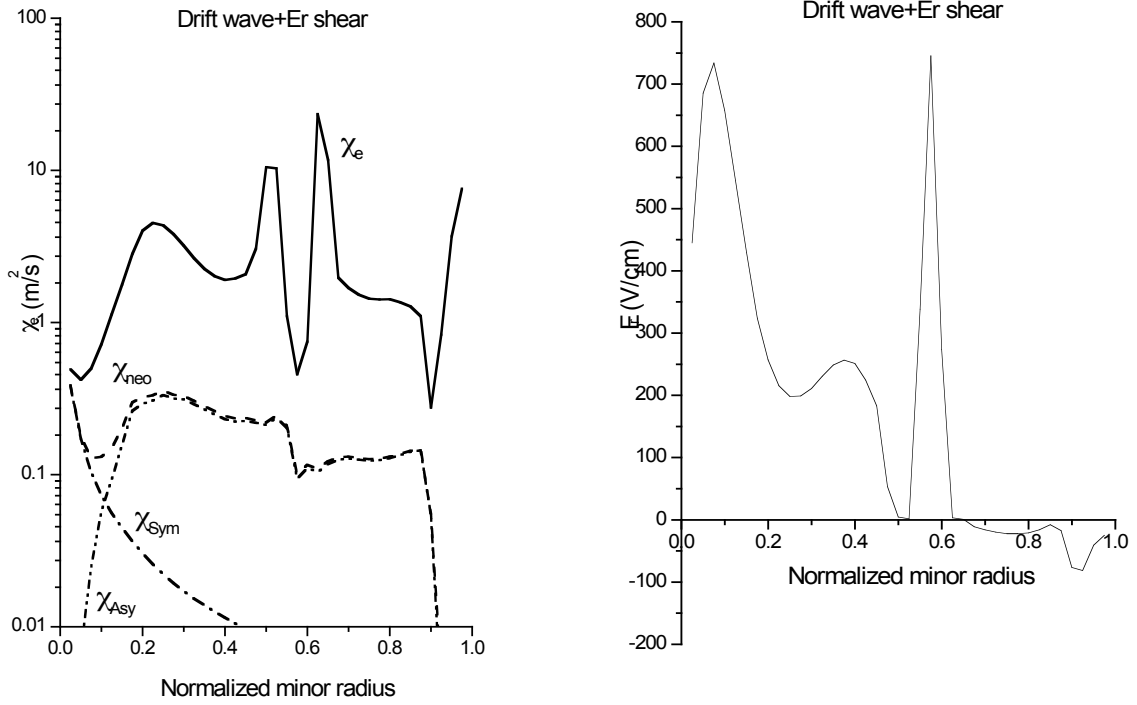

Figure 10 Electron thermal diffusivity χ_e obtained with eq.7, asymmetric neoclassical diffusivity χ_{Asy}, symmetric neoclassical diffusivity χ_{Sym} and total neoclassical diffusivity χ_{neo} (left). Electric field obtained with this model (right).

Comparing these results with the analysis of the fixed experimental profiles of the shot #26943 [19], we can conclude that the results fits reasonably well with the experimental studies.

As for the thermal diffusivities, differences between both models are more significant. Comparing the results from figures 10 and 11, one can see that for both simulations the electron thermal diffusivity is small in the region $0 \le \rho < 0.1$, and grows up to $\chi_e \approx 6$ m/s^2 in the drift wave case and up to $\chi_e \approx 10$ m/s^2 in the GyroBohm-like case in the region $0.1 \le \rho < 0.2$. After that, it drops again in the range to $0.2 \le \rho < 0.4$. This behaviour is the one expected from an ITB scenario [1]. However, although in both cases the electron thermal diffusivity is higher than the neoclassical one, in the case of drift

wave simulation, both type of transport seem to be are comparable in the region $0 \leq \rho < 0.1$, whereas for the GyroBohm-like simulation they are not. This feature is closely related to the shape of the electron temperature at the plasma core. In the drift wave case it is very peaked with a high temperature gradient in the whole range $0 \leq \rho < 0.2$, while in the GyroBohm-like case, the shape is parabolic.
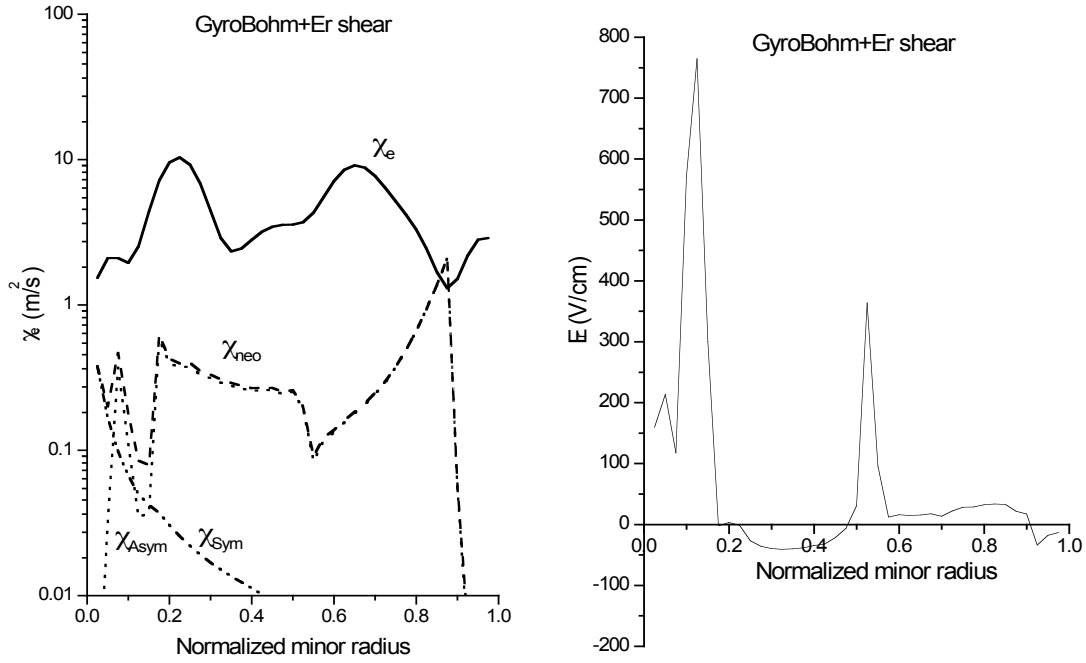

Figure 11 Electron thermal diffusivity χ_e obtained with eq.1, asymmetric neoclassical diffusivity χ_{Asy}, symmetric neoclassical diffusivity χ_{Sym} and total neoclassical diffusivity χ_{neo} (left). Electric field obtained with this model (right).

The issue of resolving what type of transport is dominant at the plasma core cannot be answered at this point because of the error bars of the experimental temperature profile. However from the dependence of the central temperature with the average density, it seems that the drift wave simulation is closer to the experimental data. Therefore, the electric field shear seems to affect the heat transport by short drift waves in a manner that reduces its value to neoclassical values or even lower than the present neoclassical model at the plasma center.

8. Profiles obtained with a non-local transport model

Usually, energy transport is described in fusion plasmas using local approaches for fluxes (particle and energy). With these models, some of the properties of the plasma related to fast responses, as propagation of sawteeth, heating power switching or impurity injection are difficult to explain. These phenomena are treated in general, adding a convective anomalous diffusivity to the conductive term, conserving, however, the local dependence on the temperature gradient.

Although a non-local model is more suitable to explain fast changes in the plasma than for steady state, it should reproduce the results of the local formalism in steady-state. In this paper, as a first step to study these non-local phenomena, a non-local heat flux transport model, based on the dependence of the heat flux in a point of the plasma with the temperature gradient of the global plasma, has been applied to solve the energy transport equation for plasmas, in absence of convective term for the anomalous transport.

The non-local model, derived for this study, used along these simulations is described in equation 10.

$$10. \qquad q_{e,ano}(r,t) = C \int n_e(r',t)\chi_{e,neo}(r',t)\nabla T_e(r',t)K(r'-r)dr'$$

With C=1 and $K(r) = \int e^{-ikr}\varphi_\alpha(a,k)dk$ being $\varphi_\alpha(a,k) = e^{-a|k|^\alpha}$ with a=1 and α =1.5. In order to take account of the reduction of heat flux due to electric field shear, the factor $1/\left(1+(\tau\omega_{ExB})^\gamma\right)$ has been used in the same way as in the previous points, obtaining the total flux as follows

$$q_e(r,t) = \frac{q_{e,ano}(r,t)}{\left(1+(\tau\omega_{ExB})^\gamma\right)}$$

In figure 12 the results of the electron temperature profile (left) as well as the dependence of the central temperature with average density (right) are given. With this model, a critical transition of the temperature is observed and some ITB scenarios are obtained. The

temperature profiles are similar to the GyroBohm-like models ones for the ITB scenarios. The central temperature dependence with average density, $T_e(0) \propto < n_e >^{-0.74}$, is also very similar to the one obtained in the GyroBohm-like case. However, in the non-ITB region, central temperature dependence with density, $T_e(0) \propto < n_e >^{-0.63}$, is higher.

The results show that, even the ITB scenarios are well simulated with this model, the global results are not so similar to the experimental ones that the previously obtained. Therefore, more studies must be done in order to use this model to analyze and simulate LHD data.
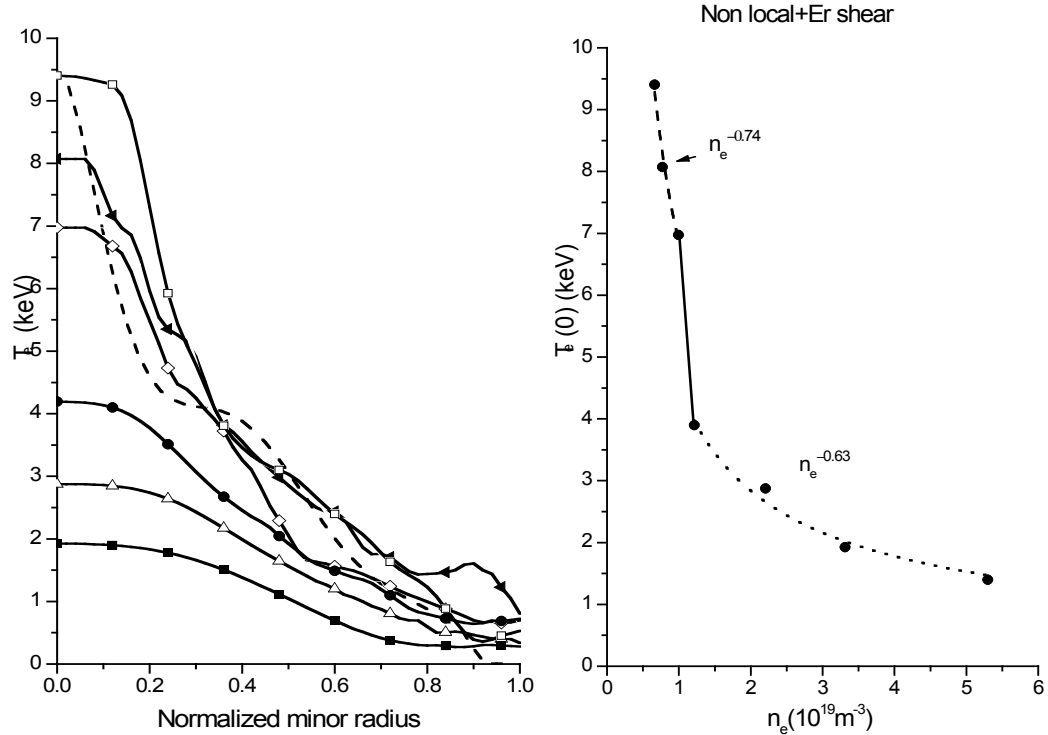

Figure 12 Electron temperature profiles obtained with equation 10 (left) and central temperature dependence with average density (right)

9. Conclusions

Some new transport models have been added to the TOTAL code for analysing the ITB formation in the LHD. The shot #26943 as well as a study of the ITB density sensitivity have been carried out.

The results show that the anomalous transport is reduced at the plasma core by the electric field shear leading to the ITB formation. The factor $\left(1 + (\tau\omega_{ExB})^{\gamma}\right)^{-1}$ introduced in the TOTAL code is able to simulate the transition between the regime with non-ITB and the ITB scenarios.

Related to the heat transport channel, it has been shown that, in the plasma core, electromagnetic drift waves are probably responsible of the anomalous transport in the ITB scenarios. With this model, the high electron temperature gradients located at the plasma core have been obtained. However, outside the central region, short drift wave models are not able to simulate electron plasma temperature because the profiles obtained have too high temperature gradients. In this region, more suitable models are related to long wavelengths models (as electrostatic drift wave or GyroBohm-like models). In this situation, a new model mixing both types of transport has been proposed. The transition location is calculated using the expression $\beta_{crit} = L_T^2 / q^2 R^2$, derived from the condition that the characteristic length of both types of transport was same. Using this model and different electron average densities with the same profile, the experimental central temperature dependence on density $T_e(0) \propto <n_e>^{-0.57}$, as well as the whole profile has been reproduced with reasonable accuracy, simulating the critical transition between non-ITB and ITB shots.

From the results previously described, a transition from large convective cells to small ones is expected at the transition from non-ITB to ITB scenarios in the plasma core when $\beta > \beta_{crit}$. However, the presence of large convective structures even at the plasma core cannot be discarded. The electron temperature profiles obtained with a GyroBohm-like model show that the critical transition between non-ITB and ITB scenarios is well simulated. However, the profiles obtained, even within the error bars, seem to be more parabolic that the experimental data. Moreover, the central temperature dependence on density, $T_e(0) \propto <n_e>^{-0.72}$, is not so similar to the experimental one like the one obtained using the electromagnetic model. However, the dependence in the non-ITB scenarios is well simulated.

These results lead to the conclusion that the reduction of anomalous transport is due to the combined effect of a high electric field with a high electric field shear and the appearance

of small convective cells due to short electromagnetic drift waves but more experimental data must be required to check it.

References

[1] Ida, K., et al., Physical Review Letters **91,** 085003 (2003)

[2] Fujisawa A. et. al. 1999 Phys. Rev. Lett. **82** 2669

[3] Castejón F. et al. Nuclear Fusion **42**, 271-280 (2002)

[4] Idei H. et al., Phy. Rev. Lett. **71**, 2220 (1993)

[5] Stroh U. et al., Phy. Rev. Lett. **86**, 5910 (2001)

[6] Yamazaki, K., Amano, T., Nuclear Fusion **32** (1992)

[7] Tala T. et al., Plasma Phys. Control. Fusion **43**, 507 (2001)

[8] Horton H. et al., New Journal of Physics **5**, (2003)

[9] Kim D. et al., Phys. Fluids, B **2**, 547-53 (1990)

[10] Jachmich J., and Weynants R.R., Plasma Phys. Control. Fusion, **42**, A147-A152 (2000)

[11] Figarella C.F. *et al.*, Phys. Rev. Lett. **90**, 015002 (2003)

[12] Itoh K. and Itoh S.I., Phys. Control. Fusion **38**, 1 (1996)

[13] Yamazaki K. et al., J. Plasma Fusion Res. SERIES, **5**, 611-615 (2002)

[14] Narihara K., Yamada I. et al., Rev. Sci. Instruments **72**, 1122 (2001)

[15] Kawahata K. et al., Rev. Sci. Instruments **70**, 707 (1999)

[16] Hinton,F.L., Hazeltine,R.D., Rev.Mod.Phys. **48**, 239(1976)

[17] Shaing,K.C., Callen,J.D., Phys Fluids **26**, 3315(1983)

[18] Chang, C.S., Hinton,F.L., Phys Fluids **25**, 1493(1982)

[19] Crume, E.C., Shaing, K.C., Hirshman, S.P., Van Rij, W.I., Phys Fluids **31**, 11(1988)